01 Jan 2006

Effects of FACTS Devices on a Power System Which Includes a Large Wind Farm

Wei Qiao

Ganesh K. Venayagamoorthy
Missouri University of Science and Technology

Ronald G. Harley

Recommended Citation

W. Qiao et al., "Effects of FACTS Devices on a Power System Which Includes a Large Wind Farm," *Proceedings of the IEEE PES Power Systems Conference and Exposition, 2006*, Institute of Electrical and Electronics Engineers (IEEE), Jan 2006.
The definitive version is available at https://doi.org/10.1109/PSCE.2006.296264

Effects of FACTS Devices on a Power System Which Includes a Large Wind Farm

Wei Qiao, *Student Member, IEEE*, Ronald G. Harley, *Fellow, IEEE*, and Ganesh K. Venayagamoorthy, *Senior Member, IEEE*

***Abstract*-- Nowadays, power systems are facing new challenges, such as increasing penetration of renewable energy sources, in particular wind generation, growing demands, limited resources, and competitive electricity markets. Under these conditions, the power systems has had to confront some major operating problems in voltage regulation, power flow control, transient stability, and damping of power oscillations, etc. Flexible AC transmission system (FACTS) devices can be a solution to these problems. This paper investigates the application of FACTS devices on a 12-bus multimachine benchmark power system including a large wind farm. A STATCOM and an SSSC are added to this power network to provide dynamic voltage control for the wind farm, dynamic power flow control for the transmission lines, relieve transmission congestion and improve power oscillation damping and transient stability.**

***Index Terms*--FACTS device, static synchronous compensator, static synchronous series compensator, wind generation**

I. Introduction

In recent years, there has been a worldwide growth in the exploitation of renewable energy, in particular wind energy. Up to now, most existing wind turbines are equipped with induction generators. In the induction generator, the amount of power converted depends on the magnitude of the grid voltage at the point of common coupling (PCC) with the grid. When a fault occurs somewhere in the grid, which causes a voltage drop at the PCC, the induction generator speeds up due to the unbalance between the mechanical shaft torque and the generator's electromagnetic torque. During this time, the induction generator draws more reactive power from the grid and contributes further to the PCC voltage collapse [1].

In the past, the amount of wind power integrated into large-scale power systems forms only a small part of the total electrical generation. Most of the electricity is still being generated by conventional sources, such as thermal, nuclear and hydro generators. Therefore, it was not necessary to require wind turbines to provide voltage and frequency support. During a large disturbance, such as a grid fault, the wind turbines are typically rapidly disconnected from the power network and reconnected when normal operation has been resumed. This is possible, as long as wind power penetration remains low. However, the penetration of wind power is increasing rapidly and is starting to influence overall power system behavior. Moreover, due to growing demands and limited resources, the power industry is facing challenges on the electricity infrastructure. As a consequence, it will become necessary to require wind farms to maintain continuous operation during grid disturbances and thereby support the network voltage and frequency.

In addition, in the era of a deregulated electricity industry, the policy of open access to transmission systems, which helped create competitive electricity markets, led to a huge increase in energy transactions over the grid and possible congestion in transmission systems. The expansion of power transfer capability of transmission systems has been a major problem over the past two decades.

Under these conditions, the modern power system has had to confront some major operating problems, such as voltage regulation, power flow control, transient stability, and damping of power oscillations, etc.

Flexible AC transmission system (FACTS) devices [2] can be a solution to these problems. They are able to provide rapid active and reactive power compensations to power systems, and therefore can be used to provide voltage support and power flow control, increase transient stability and improve power oscillation damping. Suitably located FACTS devices allow more efficient utilization of existing transmission networks.

Among the FACTS family, the shunt FACTS devices such as the static synchronous compensator (STATCOM) [2] has been widely used to provide smooth and rapid steady state and transient voltage control at points in the network. The application of a STATCOM on a wind farm equipped with doubly fed induction generators (DFIGs) to ride through grid disturbances in a single machine infinite bus (SMIB) system have been investigated in [3].

Series FACTS devices, such as the static synchronous series compensator (SSSC) [4]-[7], on the other hand, can regulate the flow of active and reactive power by injecting a controllable capacitive or inductive impedance compensation into a line at the point of connection. In addition, with a suitably designed damping controller, the SSSC has an excellent performance in damping low frequency power oscillations in a power network [6], [7].

This work was supported in part by the National Science Foundation, Washington, DC, USA, under grant ECS 0524183 and the Duke Power Company, Charlotte, North Carolina, USA.

Wei Qiao and Ronald G. Harley are with the Intelligent Power Infrastructure Consortium (IPIC) in the School of Electrical and Computer Engineering, Georgia Institute of Technology, Atlanta, GA 30332-0250 USA (e-mail: {weiqiao, rharley}@ece.gatech.edu). Ronald G. Harley is also a professor emeritus at the University of KwaZulu-Natal, Durban, South Africa.

Ganesh K. Venayagamoorthy is with the Real-Time Power and Intelligent Systems Laboratory in the Department of Electrical and Computer Engineering, University of Missouri-Rolla, Rolla, MO 65409-0249 USA (e-mail: gkumar@ieee.org).

In this paper, one generation unit in a 4-machine 12-bus benchmark power system [8] is replaced by a large wind farm equipped with DFIGs. A STATCOM and an SSSC are added to the power network to provide dynamic voltage control for the wind farm, dynamic power flow control for the transmission lines, relieve transmission congestion and improve power oscillation damping. Simulation results show that the FACTS devices significantly improve the performance of the wind farm and the power network during transient disturbances.

II. Power System Model

The original 4-machine 12-bus benchmark power system in [8] is proposed as a platform system for studying FACTS device applications and integration of wind generation. Figure 1 shows the single-line diagram of the extended 4-machine 12-bus power system which now includes a large wind farm, a STATCOM and an SSSC. The system consists of six 230-kV busses, two 345-kV busses and four 22-kV busses. It covers three geographical areas. Area 1 is predominantly a generation area with most of its generation coming from hydro power (represented by G1 and G2). Area 2, located between the main generation area (Area 1) and the main load center (Area 3), has a large wind farm (represented by G4) but is insufficient to meet local demand. Area 3, situated about 500 km from Area 1, is a load center with some thermal generation (represented by G3) available. Furthermore, since the generation unit in Area 2 has limited energy available, the system demand must often be satisfied through transmission. The transmission system consists of 230-kV transmission lines except for one 345-kV link between Areas 1 and 3 (between busses 7 and 8). Areas 2 and 3 have switched shunt capacitors to support the voltage. The detailed parameters of the system components are given in [8]. The specified voltage and the amount of active power generation at each generator bus, the load and shunt compensation at each load bus for the basic case (without the STATCOM and the SSSC) are shown in Table I.

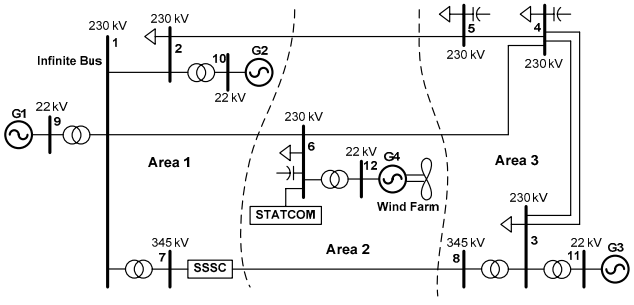

Fig. 1. Single-line diagram of the 12-bus power system incorporated with a large wind farm, a STATCOM and an SSSC.

A STATCOM is placed at bus 6 to provide steady state as well as transient voltage support for the wind farm. This dynamic reactive power compensator enhances the capability of the wind farm to ride through the grid disturbances and therefore achieve the desirable uninterrupted operation.

As discussed in [8], power flow studies on this 12-bus system reveal that in the event of a loss of generation in Area 3, or a loss of the transmission line between busses 4 and 5, line 1-6 is overloaded while the transmission capacity of the parallel path through the 345-kV transmission line 7-8 is underutilized. This congestion can be relieved by placing an SSSC at one end of line 7-8 close to bus 7. In addition, with a suitably designed damping controller, the SSSC can significantly improve power oscillation damping of the system, especially speed oscillation damping of G4 during various transient disturbances.

G1 is modeled as a three-phase infinite source, while other two conventional generators(G2 and G3) are modeled in detail, with the automatic voltage regulator (AVR), exciter and turbine governor dynamics taken in to account. The system is simulated in PSCAD/EMTDC environment.

TABLE I
Bus Data

Bus	Nominal Voltage (kV)	Specified Voltage (pu)	Load (MVA)	Shunt (MVar)	Generation (MW)
1	230				
2	230		280 + j200		
3	230		320 + j240		
4	230		320 + j240	160	
5	230		100+ j60	80	
6	230		440 + j300	180	
7	345				
8	345				
9	22	1.04			
10	22	1.02			500
11	22	1.01			200
12	22	1.02			300

III. Wind Farm Model

The wind farm is represented by an aggregated model in which over one hundred individual wind turbines and DFIGs are modeled as one equivalent DFIG driven by a single equivalent wind turbine [1]. Each individual wind turbine and DFIG represents a 3.6 MW wind turbine generator system [9]. The parameters of the equivalent wind turbine and DFIG are given in the Appendix.

The basic configuration of a DFIG driven by a wind turbine is shown in Fig. 2. The wound-rotor induction machine in this configuration is fed from both stator and rotor sides. The stator is directly connected to the grid while the rotor is fed through a partial-load variable frequency converter (VFC), which only needs to handle a fraction (25-30%) of the total power to achieve full control of the generator. In order to produce electrical power at constant voltage and frequency to the utility grid over a wide operating range from subsynchronous to supersynchronous speed, the power flow between the rotor circuit and the grid must be controlled both in magnitude and in direction. Therefore, the VFC consists of two four-quadrant IGBT PWM converters connected back-to-back by a dc-link capacitor [10]. Both converters are fully represented by individual IGBT switches and the switching frequency is 2 kHz. The IGBT switches, dc-link capacitor and other components of the VFC are built with the standard

component models from the PSCAD/EMTDC library. The crow-bar is used to short-circuit the RSC in order to protect the rotor-side converter (RSC) from over-current in the rotor circuit during grid faults.

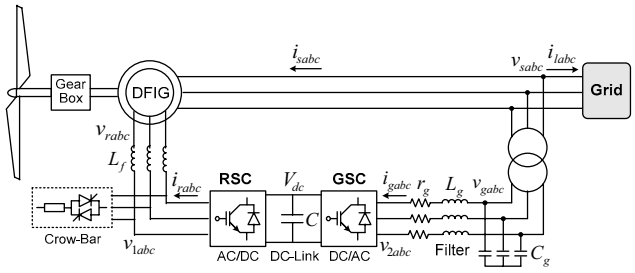

Fig. 2. Configuration of a DFIG driven by a wind turbine.

Control of the VFC includes the RSC control and the grid-side converter (GSC) control [1], [3], [10]. The objective of the RSC is to govern both the stator-side active and reactive powers independently. Figure 3 shows the overall vector control scheme of the RSC. In order to achieve independent control of the stator active power P_s (by means of speed control) and reactive power Q_s by means of rotor current regulation, the instantaneous three-phase rotor currents i_{rabc} are sampled and transformed to *d-q* components i_{dr} and i_{qr} in the stator-flux oriented reference frame. Subsequently, Q_s and P_s (thus the generator rotor speed ω_r) can be represented as functions of the individual current components. Therefore, the reference values of i_{dr} and i_{qr} can be determined directly from the Q_s and ω_r commands. The actual *d-q* current signals (i_{dr} and i_{qr}) are then compared with their reference signals (i_{dr}^* and i_{qr}^*) to generate the error signals, which are passed through two PI controllers to form the voltage signals v_{dr1} and v_{qr1}. The two voltage signals (v_{dr1} and v_{qr1}) are compensated by the corresponding cross coupling terms (v_{dr2} and v_{qr2}) to form the *d-q* voltage signals v_{dr} and v_{qr}. They are then used by the PWM module to generate the IGBT gate control signals to drive the IGBT converter.

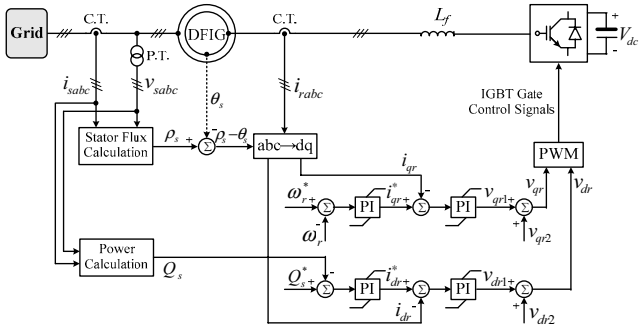

Fig. 3. Overall vector control scheme of the rotor-side converter: $v_{dr2} = -s\omega_s\sigma L_r i_{qr}$, $v_{qr2} = s\omega_s(\sigma L_r i_{dr} + L_m^2 i_{ms}/L_s)$, $\sigma = 1 - L_m^2/L_sL_r$.

The objective of the GSC is to keep the dc-link voltage constant regardless of the magnitude and direction of the rotor power. In this paper, the GSC control scheme is also designed to regulate the reactive power. This might be necessary to keep the voltage within the desired range, when the DFIG feeds into a weak power system without any local reactive compensation. When the DFIG feeds into a strong power system, the reactive power command of Q_g can simply be set to zero. Figure 4 shows the overall control scheme of the GSC. The actual signals of the dc-link voltage and the reactive power (V_{dc} and Q_g) are compared with their commands (V_{dc}^* and Q_g^*) to form the error signals, which are passed through the PI controllers to generate the reference signals for the *d*-axis and *q*-axis current components (i_{dg}^* and i_{qg}^*), respectively. The instantaneous ac-side three-phase current of the GSC are sampled and transformed into *d*-axis and *q*-axis current components i_{dg} and i_{qg} by applying the synchronously rotating reference frame transformation. The actual signals (i_{dg} and i_{qg}) are then compared with the corresponding reference signals to form the error signals, which are passed through two PI controllers. The voltage signals (v_{dg1} and v_{qg1}) are compensated by the corresponding cross coupling terms to form the *d-q* voltage signals v_{dg} and v_{qg}. They are then used by the PWM module to generate the IGBT gate control signals to drive the IGBT converter.

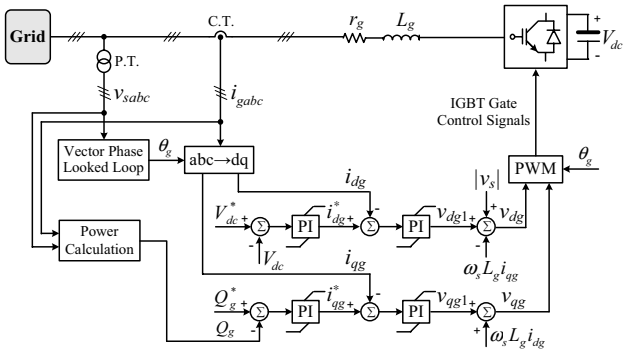

Fig. 4. Overall control scheme of the grid-side converter.

In transient stability studies, the wind turbine generator shaft system should be represented by a two-mass model instead of a single lumped-mass model [1]. The mechanical power of the turbine extracting from the wind is calculated by [1], [9]

$$P_m = \tfrac{1}{2}\rho A_r v_w^3 C_P(\lambda,\beta) \quad (1)$$

where ρ is the air density; $A_r = \pi R^2$ is the area swept by the rotor blades; v_w is the wind speed; C_P is the power coefficient, which is a function of both tip speed ratio λ and the blade pitch angle β. The C_P-λ-β curves depend on the blade design and are given by the wind turbine manufacturer.

IV. FACTS DEVICES

The STATCOM and the SSSC are each modeled as a PWM voltage-source converter, using GTO thyristors in appropriate multi-phase circuit configuration with a dc-link capacitor. The basic principles of these two FACTS devices and their control schemes are discussed in this section.

A. Static Synchronous Compensator (STATCOM)

A STATCOM [2], [11], [12], also known as an advanced static VAR compensator, is a shunt connected FACTS device.

It generates a set of balanced three-phase sinusoidal voltages at the fundamental frequency, with rapidly controllable amplitude and phase angle. A typical application of this type of controller is voltage support. In this paper, the objective of the STATCOM is to regulate the voltage at the PCC (bus 6 in Fig. 1) rapidly over the desired range and keep the dc-line voltage constant. It can enhance the capability of the wind farm to ride through transient disturbances in the grid. The overall control scheme of the STATCOM is shown in Fig. 5.

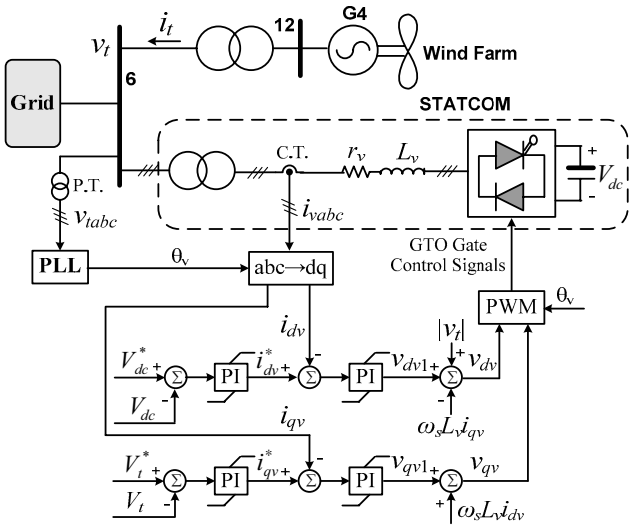

Fig. 5. Overall control scheme of the STATCOM

B. Static Synchronous Series Compensator (SSSC)

An SSSC is a series FACTS device which is connected in series with the transmission line and injects a controllable voltage in quadrature with the line current. This is equivalent to providing a controllable capacitive or inductive reactance compensation independent of the line current. Moreover, an SSSC with a properly designed damping controller can also be used to improve the damping of the low-frequency power oscillations in a power network.

In [5], Rigby and Harley reported an internal control scheme for an SSSC based on a voltage source PWM converter. By extending this work, they also proposed a power oscillation damping scheme by applying a suitably designed conventional external linear controller (CONVEC) to the SSSC [6].

The schematic diagram of the internal control scheme for the SSSC is shown in Fig. 6. The main objectives of this internal control scheme are to ensure that the injected controllable voltage at the ac terminals of the inverter remains in quadrature with the transmission line current, as well as keeping the dc terminal voltage of the inverter constant at steady state. The detailed description of the internal controller is given in [5].

The objective of the CONVEC (Fig. 7) is to damp the transient power oscillations of the system. This external controller is able to rapidly change the compensating capacitive reactance X_C injected by the SSSC, thus providing a supplementary damping torque during transient power swings [6], [7].

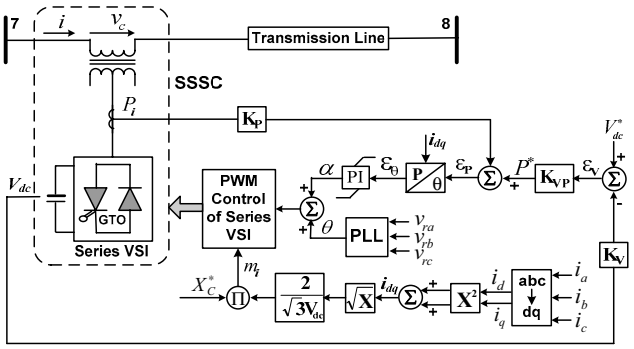

Fig. 6. Schematic diagram of the SSSC internal controller

It was reported in [13] that the speed deviation $\Delta\omega$ of a generator can be used to produce the supplementary control signal ΔX_C from the external control. In this paper, the SSSC is located on line 7-8 which connects G3 to the infinite bus. Therefore, the speed deviation $\Delta\omega_3$ of G3 should be a good input signal to the CONVEC. However, in a practical controller, it is usually desirable to choose a local signal, hence the active power deviation ΔP_{78} on line 7-8 (measured at bus 7 side), instead of the remote signal $\Delta\omega_3$, is used as the input signal to the CONVEC. In Fig. 7, ΔP_{78} is passed through two first-order low-pass filters and a damping controller (consisting of a proportional gain and a washout filter) [6], [7] to form a supplementary control signal ΔX_C, which is then added to a steady state fixed set-point value X_{C0} to form the total commanded value of compensating reactance X_C^* at the input of the internal control for the SSSC.

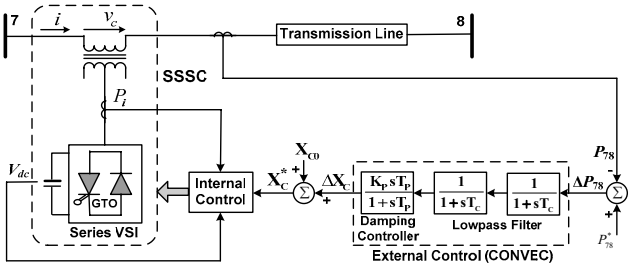

Fig. 7. Schematic diagram of the SSSC external damping controller

The damping performance of the CONVEC depends on the proportional gains K_P of the damping controller. The value of K_P is determined by evaluating the damping of oscillations after a severe fault [6], [7] as well as taking into account the operating range of the SSSC. In this paper, the value of K_P = 50 is used for several case studies in section V. The time constants in CONVEC are chosen as T_C = 1.0 s and T_P = 0.1 s.

V. Simulation Results

Simulation studies are carried out in this section to investigate the effects of the FACTS devices on the 12-bus power system including a large wind farm. The system is exposed to various transient disturbances, and the system responses, reinforced with the FACTS devices, are compared with the original system. For all cases, the set-point value of

the compensating reactance of the internal controller (Fig. 7) is chosen as X_{C0} = 60 ohm when the SSSC is connected to the system.

A. Transmission Congestion Relief by the SSSC

For the power system in Fig. 1, if line 4-5 is open, the load demands in Area 3 are mainly supplied by generation in Area I through two transmission lines: line 1-6 and line 7-8. Due to the low capacity limit (250MVA) of line 1-6, the loss of line 4-5 results in the overloading of line 1-6 while the transmission capacity (500 MVA) of line 7-8 is underutilized. The shortage of transmission capacity of line 1-6 causes transmission congestion between Areas 1 and 3. This problem can be relieved by using an SSSC on line 7-8 to dynamically change the total line reactance to regulate the transmitted active power through line 7-8, and therefore relieve the overloading of line 1-6.

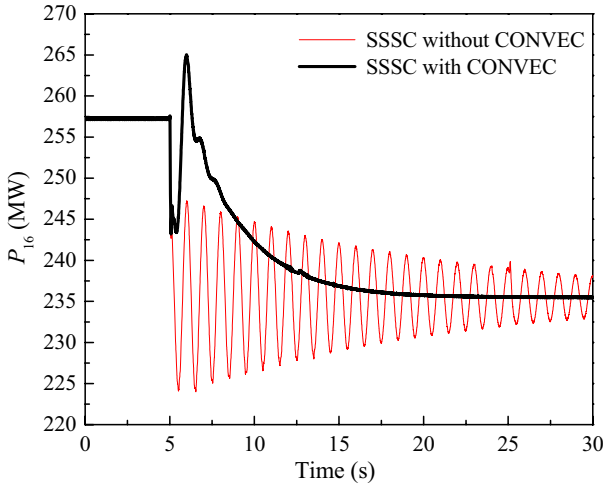

Fig. 8. The active power delivered by line 1-6: P_{16} (MW)

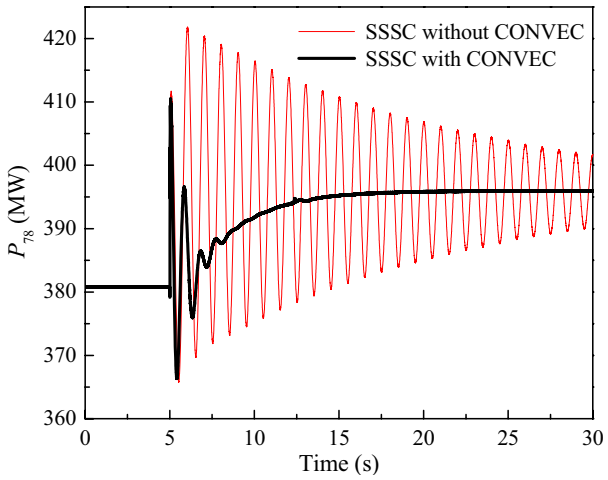

Fig. 9. The active power delivered by line 7-8: P_{78} (MW)

It is assumed that line 4-5 is open during the entire test and the SSSC is connected to line 7-8 at t = 5.0 s. The active power reference value P_{78}^* of the external controller is set at 395 MW. Figures 8 and 9 show the results of the active power delivered by line 1-6 (P_{16}) and line 7-8 (P_{78}), respectively. Before applying the SSSC, the active power delivered by line 1-6 is 257 MW, which exceeds the capacity limit of line 1-6. Applying the SSSC reduces the active power flow of line 1-6 to 235 MW while increasing the active power flow of line 7-8 from 381 MW to 395 MW. In addition, the power oscillations of line 1-6 and line 7-8 are weakly damped without the use of the external damping controller CONVEC. The CONVEC improves the damping of power oscillations significantly. Therefore, the SSSC with the CONVEC can quickly regulate the active power of line 7-8 (also line 1-6) to the steady state set-point value.

B. A Three-Phase Short Circuit Test on Line 1-6

The use of the STATCOM to improve the wind farm dynamic performance during the transient state is evaluated in this subsection. The 12-bus system is operated with the SSSC and with/without the STATCOM. If there is no STATCOM, the reactive power command of the RSC in Fig. 3, Q_r^*, is set to 156 MVar in order to control the voltage of bus 6 (PCC) to the desired value.

A 150 ms three-phase short circuit is applied to the bus 1 end of line 1-6 at t = 5 s. Figures 10 and 11 show the results of the rotor active power, P_r, and the rotor reactive power, Q_r, respectively. With a STATCOM to provide the dynamic reactive compensation, the rotor power of the DFIG is within the limit of the VFC power capacity (25% of the DFIG rated power) during the post-fault transient state. However, if there is no STATCOM, the rotor power of the DFIG exceeds the limit of the VFC power capacity with large oscillations. The VFC has to be blocked or disconnected from the system. As a result, the wind farm might be tripped out.

Fig. 12 shows the voltage profiles of bus 6 with and without the STATCOM. With the STATCOM for voltage control, the voltage drop and oscillation during and after this grid fault are much smaller than without the STATOCM. These results indicate that the STATCOM is effective for dynamic voltage control at the PCC where the wind farm is connected to the power network. The STATCOM significantly enhances the capability of wind farm to ride through the grid disturbances.

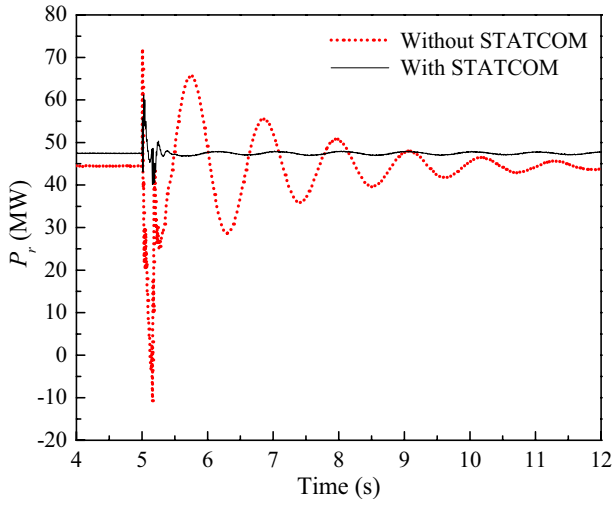

Fig. 10. The rotor active power of the DFIG G4: P_r (MW)

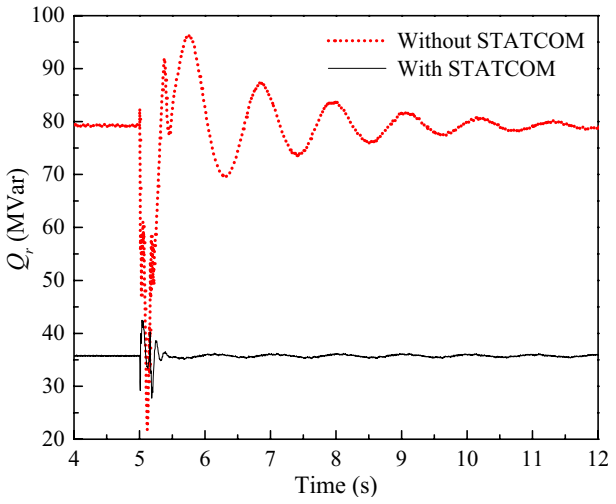

Fig. 11. The rotor reactive power of the DFIG G4: Q_r (MVar)

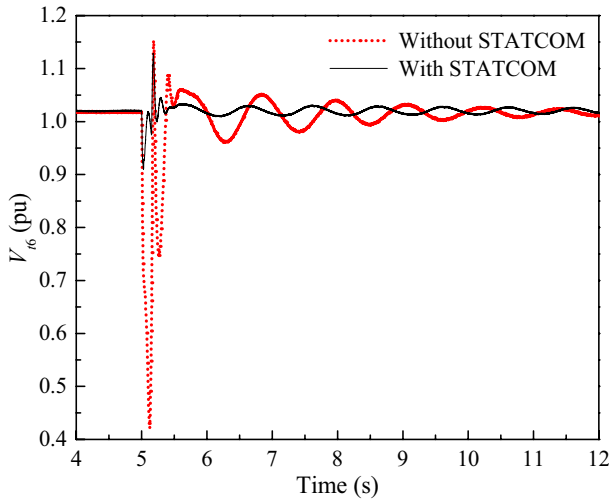

Fig. 12. The terminal voltage of bus 6: V_{t6} (pu)

C. A Three-Phase Short Circuit Test on Line 7-8

The system in Fig. 1 is operated with the STATCOM and the SSSC. Line 4-5 is closed during the entire test. A 150 ms three-phase short circuit is applied to the bus 7 end of line 7-8 at t = 5 s. Figures 13 and 14 show the results of the rotor angle of G3, ω_3, and the active power delivered by line 7-8, P_{78}, respectively. These results indicate that with the CONVEC, the system oscillations are quickly damped out in only two or three cycles. However, without the CONVEC, the system only provides slight damping to these oscillations.

D. A Three-Phase Short Circuit Test on Line 7-8 with the Loss of Line 4-5

The dynamic damping performance of the CONVEC is now evaluated at another operating point, where the system is operated with the STATCOM and the SSSC but line 7-8 is now open during the entire test. The same 150 ms three-phase short circuit as in Subsection C is applied to the bus 7 end of line 7-8 at t = 5 s. Figures 15 and 16 show the rotor angle of G3, ω_3, and the active power delivered by line 7-8, P_{78}, respectively. Again, these results show that the CONVEC provides the effective damping to the post-fault oscillations of the system.

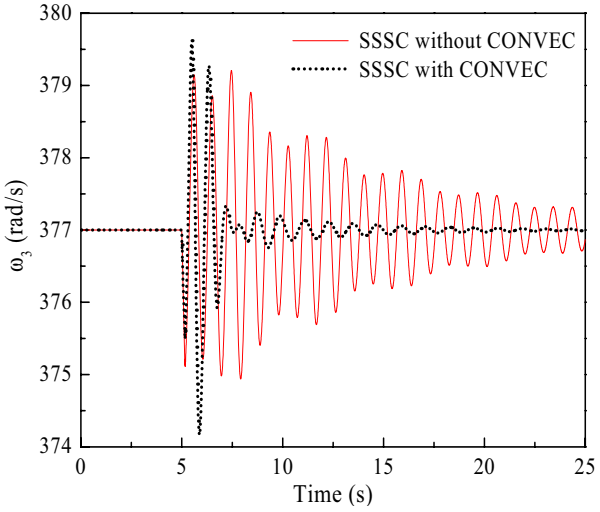

Fig. 13. The rotor angle of G3: ω_3 (rad/s)

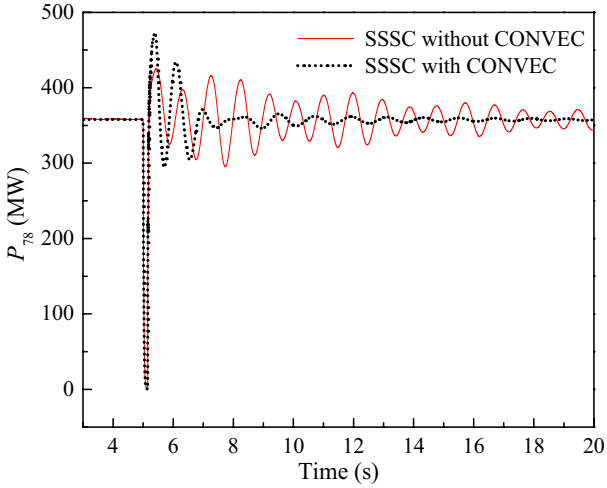

Fig. 14. The active power delivered by line 7-8: P_{78} (MW)

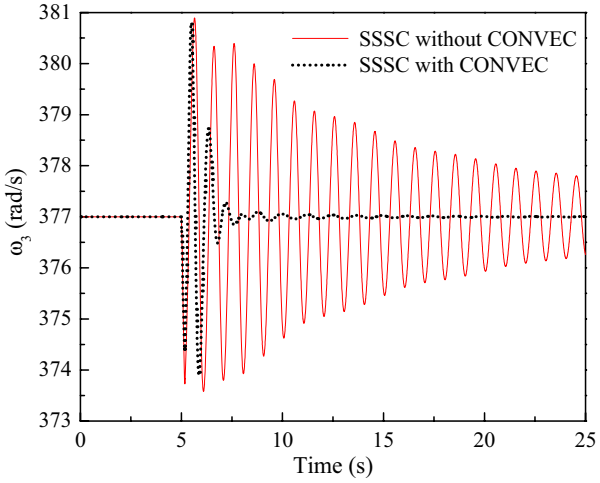

Fig. 15. The rotor angle of G3: ω_3 (rad/s)

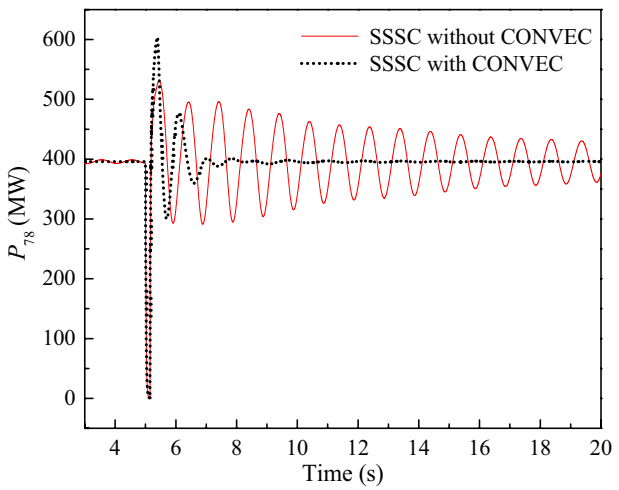

Fig. 16. The active power delivered by line 7-8: P_{78} (MW)

VI. Conclusion

The increasing penetration of renewable energy sources, growing demands, limited resources, and deregulated electricity markets has caused new challenges to the operation, control and stability of modern electric power systems. This paper investigates the application of FACTS devices to enhance the dynamic and transient performance of power systems which includes a large wind farm. A STATCOM and an SSSC are placed at suitable locations in a 12-bus multimachine power system with a large wind farm. Results show that the FACTS devices provide an effective means in dynamic voltage control of the wind farm, enhancing the capability of the wind farm to ride through the grid disturbances, dynamic power flow control of the transmission lines, relieving transmission congestion, and improving power oscillation damping and transient stability.

VII. Appendix

Wind turbine: rated capacity = 400 MW, number of blades = 3, rotor diameter = 104 m, swept area = 8495 m^2, rotor speed (variable) = 8.5-15.3 rpm.

Induction generator (on a 400 MW base): rated power = 400 MW, rated stator voltage = 22 kV, r_s = 0.0079 pu, r_r = 0.025 pu, L_{ls} = 0.07937 pu, L_{lr} = 0.40 pu, L_m = 4.4 pu.

VIII. References

[1] V. Akhmatov, "Analysis of Dynamic Behavior of Electric Power Systems with Large Amount of Wind Power," Ph.D. dissertation, Technical University of Denmark, Kgs. Lyngby, Denmark, Apr. 2003.

[2] N. G. Hingorani and L. Gyugyi, *Understanding FACTS: Concepts and Technology of Flexible AC Transmission Systems*, IEEE, New York, 2000, ISBN 0-7803-3455-8.

[3] W. Qiao, G. K. Venayagamoorthy, and R. G. Harley, "Real-time implementation of a STATCOM on a wind farm equipped with doubly fed induction generators," to be presented at the *IEEE IAS 41th Annual Meeting*, Tampa, FL, USA, Oct. 8-12, 2006.

[4] L. Gyugyi, C. D. Schauder, and K. K. Sen, "Static synchronous series compensator: a solid-state approach to the series compensation of transmission lines," *IEEE Trans. Power Delivery*, vol. 12, no. 1, Jan. 1997, pp. 406-417.

[5] B. S. Rigby and R. G. Harley, "An improved control scheme for a series-capacitive reactance compensator based on a voltage-source inverter," *IEEE Trans. Industry Applications*, vol. 34, no. 2, pp. 355-363, Mar./Apr. 1998.

[6] B. S. Rigby, N. S. Chonco, and R. G. Harley, "Analysis of a power oscillation damping scheme using a voltage-source inverter," *IEEE Trans. Industry Applications*, vol. 38, no. 4, July/Aug. 2002, pp. 1105-1113.

[7] W. Qiao and R. G. Harley, "Indirect adaptive external neuro-control for a series capacitive reactance compensator based on a voltage source PWM converter in damping power oscillations," *IEEE Trans. Industrial Electronics*, accepted for future publication.

[8] S. Jiang, U. D. Annakkage, and A. M. Gole, "A platform for validation of FACTS models," *IEEE Trans. Power Delivery*, vol. 21, no. 1, Jan. 2006, pp. 484-491.

[9] N. W. Miller, W. W. Price, and J. J. Sanchez-Gasca, "Dynamic modeling of GE 1.5 and 3.6 wind turbine-generators," GE-Power Systems Energy Consulting, General Electric International, Inc., Schenectady, NY, USA, Oct. 27, 2003.

[10] R. Pena, J. C. Clare, and G. M. Asher, "Doubly fed induction generator using back-to-back PWM converters and its application to variable-speed wind-energy generation," *IEE Proceedings – Electric Power Applications*, vol. 143, no. 3, May 1996, pp. 231-241

[11] C. Schauder and H. Mehta, "Vector analysis and control of advanced static VAR compensators," *IEE Proceedings – Generation, Transmission and Distribution*, vol. 140, no. 4, Jul. 1993, pp. 299-306.

[12] P. Rao, M. L. Crow, and Z. Yang, "STATCOM control for power system voltage control applications," *IEEE Trans. Power Delivery*, vol. 15, no. 4, Oct. 2000, pp. 1311-1317.

[13] F. J. Swift and H. F. Wang, "Application of the controllable series compensator in damping power system oscillations," *IEE Proc. Generation, Transmission and Distribution*, vol. 143, no. 4, pp. 359-364, July 1996.